Structural Engineering and Mechanics, Vol. 7, No. 3 (1999) 331-344
DOI: http://dx.doi.org/10.12989/sem.1999.7.3.331

Transient response of a right-angled bent cantilever subjected to an out-of-plane tip load

B. Wang†

School of Engineering and Technology, Deakin University, Victoria 3217, Australia

G. Lu‡

School of Mechanical and Manufacturing Engineering, Swinbourne University of Technology, Victoria 3122, Australia

Abstract. This paper provides an analysis of the transient behaviour of a right-angled bent cantilever beam subjected to a suddenly applied force at its tip perpendicular to its plane. Based on a rigid, perfectly plastic material model, a double-hinge mechanism is required to complete the possible deformation under a rectangular force pulse (constant force applied for a finite duration) with a four-phase response mode. The kinematics of the various response phases are described and the partitioning of the input energy at the plastic hinges during the motion is evaluated.

Key words: impulsive load; dynamic plasticity; inertia effect; plastic hinge.

1. Introduction

An understanding of the response of engineering structures and components under impact loading is of practical importance in assessing the safety of nuclear power stations, chemical plants and other industrial establishments which could be exposed to potentially accidental explosions or damages to various critical components when struck by energetic objects. For instance, in a nuclear power station, a sudden rupture of a high pressure piping system is a safety related matter. If such a sudden break happens, the magnitude of the reaction force (the blow-down force) from the leaking fluid can be substantial and consequently cause a whipping motion. The pipe will undergo dynamic plastic deformation and could acquire considerable kinetic energy. This is termed pipe whip.

Modeling the mechanics of a whipping pipe is a complex problem. It can be solved at various levels of complexity. The simplest approach is to formulate a small deflection, rigid-plastic analysis in which the pipe is treated as a cantilever beam subjected to a suddenly applied end load. The effect of geometrical changes and material elasticity are neglected. This approach remains the fundamental basis of an initial approach to some particular problems in pipe whip research.

Recently, attention has been given to response of a two-dimensional piping system subjected to

† Lecturer
‡ Senior Lecturer

suddenly applied forces at its tip perpendicular to its plane. Amongst various engineering configurations, right-angled bent pipes are of particular interest for their wide applications in practice. The complete range of possible deformation mechanisms for an impulsive loading and a step force was described by Wang (1994) and Reid, Wang and Yu (1995), respectively. They showed that various failure modes may occur with the maximum of two plastic hinges appearing simultaneously in the cantilever pipe.

Under an out-of-plane tip load F, as shown in Fig. 1, segment AC of a right-angled bent cantilever is under pure bending, and CB is under combined bending and torsion. A simple static analysis yields that when $F \leq F_0$, where

$$F_0 = \frac{M_0}{L_2\sqrt{1+(M_0/T_0)^2(L_1/L_2)^2}},$$

there will be no failure in the beam, M_0 and T_0 being the dynamic fully plastic bending moment and torque of the beam, L_1 and L_2 being the lengths of segments AC and CB, respectively. Reid, Wang and Yu (1995) showed that for a step load, there is a limiting force magnitude F_2. When $F_0 \leq F < F_2$, only one combined bending-torsion hinge will be formed in the beam either at B or in CB, i.e., a single hinge mechanism; when $F \leq F_2$, a double-hinge mechanism will apply with a pure bending hinge in AC and a combined bending-torsion hinge in CB simultaneously. Since a step load is time independent, the hinges are stationary in the beam during the deformation. In this paper, the transient behaviour is examined for a right-angled bent cantilever subjected to an out-of-plane rectangular pulse. It is shown that when the applied force is removed, the plastic hinges start to travel along the beam segments. The kinematics of the travelling hinges, the response time of the cantilever, the deflection of its tip and the energy partitioning at various times are all features of the motion to be studied. The cantilever ultimately comes to rest after a final root rotation phase. Attention herein is focused on the cases corresponding to high load magnitude when a double-hinge mechanism is initiated since this response contains all of the features which might occur for this type of problem.

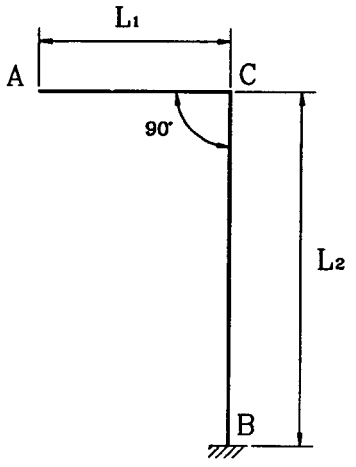

Fig. 1 A right-angled bent cantilever

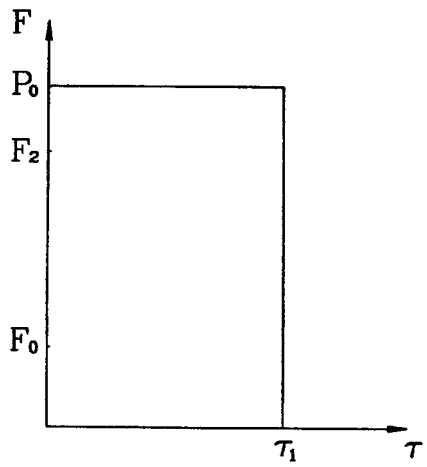

Fig. 2 The rectangular pulse of finite duration

2. Theoretic modeling

Consider a cantilever comprised of two straight segments of length L_1 and L_2, shown in Fig. 1. The cantilever is loaded normally to its plane by a rectangular force pulse at its tip. The pulse can be represented as

$$F = \begin{cases} P_0 & 0 \le \tau \le \tau_1 \\ 0 & \tau_1 < \tau \end{cases}$$

as shown in Fig. 2. It is assumed in this paper that the beam is made from a rigid, perfectly plastic material, the beam's deflection is small and the analysis is referred to its original configuration. Under a combined bending-torsional deformation, the yield criterion is given as

$$\left(\frac{M}{M_0}\right)^2 + \left(\frac{T}{T_0}\right)^2 = 1 \tag{1}$$

with an associated flow rule,

$$\dot{\varphi} = \left(\frac{M_0}{T_0}\right)^2 \frac{T}{M}\,\dot{\vartheta} \tag{2}$$

Also, the ratio of T/M is assumed to be less than 1 as it is the case for most of the engineering beam structures. For those with T/M=1, an analysis was given by Martin (1964) for an impulsive loading condition. It showed a pure bending then pure torsion single hinge mechanism, a solution very similar to that of an equivalent straight beam solved by Parkes (1955); for those with $T/M > 1$ under step loads, Hua *et al.* (1988) provided a double-hinge solution different from that in this paper.

2.1. Double-hinge mechanism (Phase I)

Assume that a pure bending hinge H_1 and a combined bending-torsion hinge H_2 are formed in segment AC and CB, respectively, as shown in Fig. 3. $\dot{\vartheta}_1$, $\dot{\vartheta}_2$ and $\dot{\varphi}_2$ are the relative angular velocities due to bending and torsion at the plastic hinges. Applying D'Alembert's principle, the governing equations of each beam segment can be obtained.

1) For segment H_1H_2, the equation of translational motion is

$$0 = -\mu x_2 \frac{x_2}{2}\,\ddot{\vartheta}_2 + \mu(L - x_1)\frac{(L - x_1)}{2}\,\ddot{\varphi}_2 - \mu(L - x_1)x_2\ddot{\vartheta}_2 \tag{3}$$

The rotational equation about axis CB is

$$M_0 - T_2 = \frac{\mu}{3}(L_1 - x_2)^3\,\ddot{\varphi}_2 - \frac{\mu}{2}(L_1 - x_1)^2 x_2 \ddot{\vartheta}_2 \tag{4}$$

where the polar inertia of segment CH_2 is neglected. And the rotational equation about axis AC is

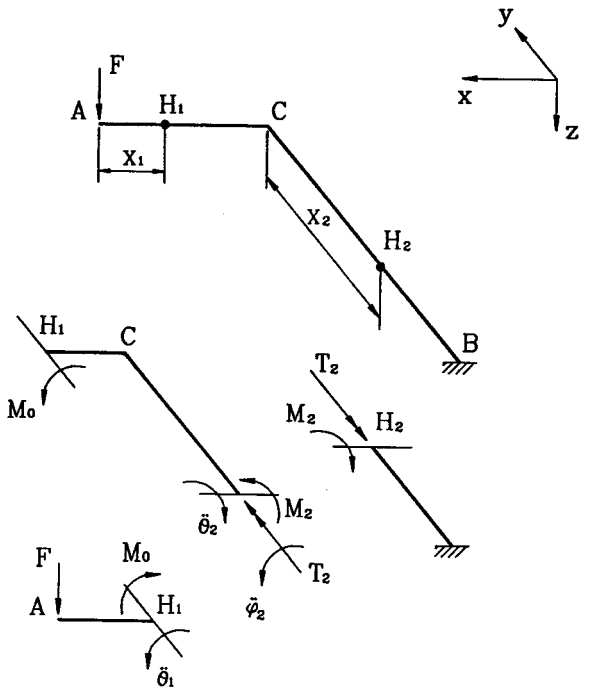

Fig. 3 Free body diagram for a double-hinge mechanism

$$M_2 = \frac{\mu}{6} x_2^3 \ddot{\vartheta}_2 \tag{5}$$

2) For segment AH_1, the equation of translational motion is

$$F = \mu x_1 \left[\frac{x_1}{2} \ddot{\vartheta}_1 + \left(L_1 - \frac{x_1}{2} \right) \ddot{\varphi}_2 - x_2 \ddot{\vartheta}_2 \right] \tag{6}$$

and the rotational equation about H_1 is

$$F x_1 - M_0 = \frac{\mu}{3} x_1^3 \ddot{\vartheta}_1 + \mu \left(\frac{L_1}{2} - \frac{x_1}{6} \right) x_1^2 \ddot{\varphi}_2 - \frac{\mu}{2} x_1^2 x_2 \ddot{\vartheta}_2 \tag{7}$$

The yield condition at hinge H_2 is

$$\left(\frac{M_2}{M_0} \right)^2 + \left(\frac{T_2}{T_0} \right)^2 = 1$$

and because the hinge does not move during the pulse, M_2 and T_2 are time independent. The flow rule becomes

$$\ddot{\varphi}_2 = \left(\frac{M_0}{T_0} \right)^2 \frac{T_2}{M_2} \ddot{\vartheta}_2 \tag{8}$$

From Eq. (3), we have

$$\ddot{\varphi}_2 = \frac{x_2^2 + 2(L_1 - x_1)x_2}{(L_1 - x_1)^2} \ddot{\vartheta}_2 \tag{9}$$

Substituting it into Eqs. (8) and (4) produces, respectively,

$$\frac{T_2}{M_2} = \left(\frac{T_0}{M_0}\right)^2 \frac{x_2^2 + 2(L_1 - x_1)x_2}{(L_1 - x_1)^2} \tag{10}$$

and

$$T_2 = M_0 - \frac{\mu}{3}(L_1 - x_1)x_2\left(x_2 + \frac{L_1 - x_1}{2}\right)\ddot{\vartheta}_2 \tag{11}$$

Then putting M_2 and T_2 into Eqs. (1) and (10) gives

$$\left[\frac{M_0 - \frac{\mu}{3}(L_1 - x_1)x_2\left(x_2 + \frac{L_1 - x_1}{2}\right)\ddot{\vartheta}_2}{T_0}\right]^2 + \left(\frac{\frac{\mu}{6}x_2^3\ddot{\vartheta}_2}{M_0}\right)^2 = 1 \tag{12}$$

and

$$\left(\frac{T_0}{M_0}\right)^2 \frac{x_2^2 + 2(L_1 - x_1)x_2}{(L_1 - x_1)^2} = \frac{M_0 - \frac{\mu}{3}(L_1 - x_1)x_2\left(x_2 - \frac{L_1 - x_1}{2}\right)\ddot{\vartheta}_2}{\frac{\mu}{6}x_2^3\ddot{\vartheta}_2} \tag{13}$$

By eliminating $\ddot{\vartheta}_1$ in Eqs. (6) and (7), we have

$$\frac{1}{3}Fx_1 - M_0 = -\frac{\mu x_1^2 x_2(L_1 - x_1 + x_2)}{6(L_1 - x_1)}\ddot{\vartheta}_2 \tag{14}$$

Eqs. (12) to (14) form a set of nonlinear equations for unknowns x_1, x_2 and $\ddot{\vartheta}_2$. Given the value of F, the equations can be solved numerically. It is noted that all variables during the pulse remain constant and this represents a stationary hinge phase. Fig. 4 shows schematically the shear force, bending moment and torque distribution along the beam segments.

The value of F_2, the minimum magnitude of F required for a double-hinge mechanism can be derived by letting $\ddot{\vartheta}_1 = 0$ in Eqs. (6) and (7), then we have

$$M_0 = \mu\left[\left(\frac{L_1}{2} - \frac{x_1}{3}\right)\frac{x_2 + 2(L_1 - x_1)}{(L_1 - x_1)^2} - \frac{1}{2}\right]x_1^2 x_2 \ddot{\vartheta}_2 \tag{15}$$

Combining Eq. (15) with Eqs. (12) and (13), we can solve the positions of H_1 and H_2 in the beam. They represent the closest positions to bend C the two hinges may possibly appear in segments AC and CB, respectively. And F_2 can be calculated by employing Eq. (6).

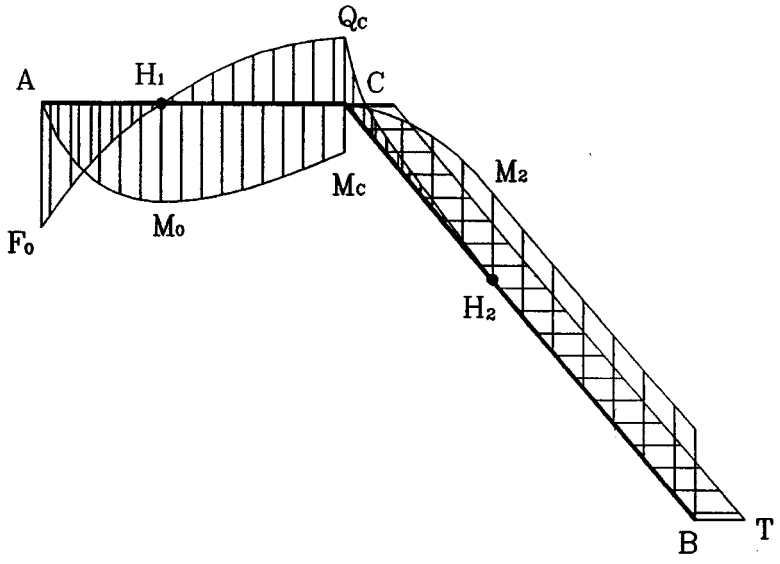

Fig. 4 Diagram of shear force, bending moment and torque distribution for a double-hinge mechanism

With subscript "*I*" denoting values at the end of Phase I, we have,

$$\dot{\vartheta}_{1I}=\ddot{\vartheta}_1\tau_1 \text{ and } \vartheta_{1I}=\frac{1}{2}\ddot{\vartheta}_1\tau_1^2$$

also

$$\dot{\vartheta}_{2I}=\ddot{\vartheta}_2\tau_1,\ \vartheta_{2I}=\frac{1}{2}\ddot{\vartheta}_2\tau_1^2,\ \dot{\varphi}_{2I}=\ddot{\varphi}_2\tau_1, \text{ and } \varphi_{2I}=\frac{1}{2}\ddot{\varphi}_2\tau_1^2.$$

Assuming small deflections, the velocity and deflection of the beam tip can be written as

$$\dot{\delta}_{AI}=x_1\dot{\vartheta}_{1I}+L_1\dot{\varphi}_{2I}-x_2\dot{\vartheta}_{2I}, \text{ and } \delta_{AI}=x_1\vartheta_{1I}+L_1\varphi_{2I}-x_2\vartheta_{2I}$$

respectively. Thus, the total energy provided by the load is

$$E=F\,\delta_{AI}.$$

And the energy dissipated at the plastic hinges in Phase I is

$$E_{II}=M_0\vartheta_{1I}+M_2\vartheta_{2I}+T_2\varphi_{2I}.$$

When the load is removed at $\tau=\tau_I$, the sudden change in shear force distribution causes both hinges H_1 and H_2 to move towards bend C, as discussed in the following text. There is a limiting position of H_1 in AC, the relative angular velocity across the hinge becomes zero when it reaches the position and AC becomes completely rigid again. This ends Phase II of the response. As soon as hinge H_1 vanishes, hinge H_2 begins to move towards B and when it reaches B, Phase III finishes. The final phase, Phase IV, consists of the whole rigid bent cantilever rotating about B until all of the remaining kinetic energy is absorbed in plastic deformation. Then the cantilever stops. Phases II to IV are described in the following.

2.2. Phase II

As soon as the load is removed, H_1 and H_2 are no longer stationary and start to travel towards C. They still remain a pure bending hinge and a combined bending-torsion one, respectively. The variables involved in this phase are x_1, x_2, ϑ_1, ϑ_2, φ_2, M_2 and T_2. The derivation of governing equations for this phase, which is shown schematically in Fig. A1, is presented in an Appendix. When the governing equations are obtained, they are reorganized into a form suitable for numerical solutions.

$$\ddot{\vartheta}_2 = \frac{6M_2}{\mu x_2^3} - \frac{9}{x_2(L_1 - x_1 + x_2)}\left[\frac{M_2}{\mu x_2^2}(L_1 - x_1 + x_2) + \frac{T_2 - M_0}{\mu(L_1 - x_1)}\right] \tag{16}$$

$$\dot{x}_2 = \frac{3}{\dot{\vartheta}_2(L_1 - x_1 + x_2)}\left[\frac{M_2}{\mu x_2^2}(L_1 - x_1 + x_2) + \frac{T_2 - M_0}{\mu(L_1 - x_1)}\right] \tag{17}$$

$$\ddot{\vartheta}_1 = \frac{3\dot{x}_2\dot{\vartheta}_2 - 12\dfrac{M_0}{\mu x_1^3}\left(L_1 - \dfrac{x_1}{2}\right) - \dfrac{3M_2}{\mu x_2^2} - \dfrac{3(M_0 - T_2)}{\mu(L_1 - x_1)^2}}{(L_1 - x_1)} \tag{18}$$

$$\ddot{\varphi}_2 = \frac{-3}{(L_1 - x_1)\left(\dfrac{L_1 - x_1}{2} + x_2\right)}\left[\left(L_1 - x_1 + \frac{x_2}{2}\right)\frac{2(T_2 - M_0)}{\mu(L_1 - x_1)^2} + \frac{x_2}{2}\dot{x}_2\dot{\vartheta}_2\right] \tag{19}$$

$$\dot{x}_1 = \frac{1}{\dot{\vartheta}_1}\left[\frac{6M_0}{\mu x_1^2} - \frac{3M_2}{\mu x_2^2} + \dot{x}_2\dot{\vartheta}_2 - \frac{3(M_0 - T_2)}{\mu(L_1 - x_1)^2}\right] \tag{20}$$

Letting $T_2/T_0=\sin\sigma$ and $M_2/M_0=\cos\sigma$, the yield condition is satisfied automatically. From the associated flow rule, we have

$$\sigma = \tan^{-1}\left(\frac{T_0\dot{\varphi}_2}{M_0\dot{\vartheta}_2}\right) \tag{21}$$

A standard fourth order Runge-Kutta procedure is employed to calculate x_1, x_2, $\dot{\vartheta}_1$, $\dot{\vartheta}_2$, $\dot{\varphi}_2$ at each time instant. At the end of each step, σ (i.e., M_2 and T_2) is then updated. When $\dot{\vartheta}_1$ becomes zero, hinge H_1 is inactive, Phase II ends and the time is denoted by τ_{II}.

2.3. Phase III

When hinge H_1 reaches its terminal position and becomes inactive, the combined bending-torsion hinge H_2 becomes the only hinge running towards root B. The equations of motion for segment ACH_2 are

$$\left(L_1 + \frac{x_2}{2}\right)x_2\ddot{\vartheta}_2 + \frac{L_1^2}{2}\ddot{\varphi}_2 + (L_1 + x_2)\dot{x}_2\dot{\vartheta}_2 = 0 \tag{22}$$

$$\frac{x_2}{2}\ddot{\vartheta}_2 + \frac{L_1}{3}\ddot{\varphi}_2 + \frac{1}{2}\dot{x}_2\dot{\vartheta}_2 = -\frac{T_2}{\mu L_1^2} \tag{23}$$

and

$$\frac{x_2}{3}\ddot{\vartheta}_2 + \dot{x}_2\dot{\vartheta}_2 = \frac{2M_2}{\mu x_2^2} \tag{24}$$

At hinge H_2, the flow rule and yield condition remain the same. Eqs. (22) to (24) can be rewritten for numerical solution,

$$\ddot{\vartheta}_2 = \frac{6M_2}{\mu x_2^3} - \frac{9}{x_2}\left[\frac{M_2(L_1+2x_2)}{\mu x_2^2(L_1+x_2)} - \frac{T_2}{\mu L_1(L_1+x_2)}\right] \tag{25}$$

$$\dot{x}_2 = \frac{3}{\dot{\vartheta}_2}\left[\frac{M_2(L_1+2x_2)}{\mu x_2^2(L_1+x_2)} - \frac{T_2}{\mu L_1(L_1+x_2)}\right] \tag{26}$$

$$\ddot{\varphi}_2 = -\left(\frac{3T_2}{\mu L_1^3} + \frac{3\dot{x}_2\dot{\vartheta}_2}{2L_1} + \frac{3x_2\ddot{\vartheta}_2}{2L_1}\right) \tag{27}$$

M_2 and T_2 can be replaced by variable σ as in Phase II. The initial values of x_2, $\dot{\vartheta}_2$, ϑ_2, $\dot{\varphi}_2$, φ_2 and σ are obtained from the end of Phase II, and Eqs. (21), and (25) to (27) can be solved numerically. Note that in this phase, the positive direction of ϑ_2 is defined as being opposite to that in Phase II. When hinge H_2 reaches the root B, Phase III ends and the time at the moment is denoted by τ_{III}.

2.4. Phase IV

After hinge H_2 arrives at B, the motion of the whole cantilever becomes a rigid body rotation about B until all of the remaining kinetic energy is dissipated at hinge H_B. With subscript "B" denoting values of the parameters at the root, the equations of motion for the whole beam can be expressed as follows,

$$\left(L_1 + \frac{L_2}{2}\right)L_2\ddot{\vartheta}_B + \frac{1}{2}L_1^2\ddot{\varphi}_B = -\frac{Q_B}{\mu} \tag{28}$$

$$\frac{L_2}{2}\ddot{\vartheta}_B + \frac{L_1}{3}\ddot{\varphi}_B = -\frac{T_B}{\mu L_1^2} \tag{29}$$

and

$$\left(L_1 + \frac{L_2}{3}\right)L_2\ddot{\vartheta}_B + \frac{1}{2}L_1^2\ddot{\varphi}_B = -\frac{M_B}{\mu L_2} \tag{30}$$

where Q_B is a shear force at the root perpendicular to axis of CB.

The flow rule and yield condition at B are

$$\dot{\varphi}_B = \left(\frac{M_0}{T_0}\right)^2 \frac{T_B}{M_B}\,\dot{\vartheta}_B \quad \text{and} \quad \left(\frac{M_B}{M_0}\right)^2 + \left(\frac{T_B}{T_0}\right)^2 = 1$$

Hence, the angular accelerations can be written as

$$\ddot{\vartheta}_B = \frac{1}{\mu L_2\left(\frac{L_1}{4}+\frac{L_2}{3}\right)}\left(\frac{3T_0}{2L_1\sqrt{1+(M_0\dot{\vartheta}_B/T_0\dot{\varphi}_B)^2}} - \frac{M_0}{L_2\sqrt{1+(T_0\dot{\varphi}_B/M_0\dot{\vartheta}_B)^2}}\right) \tag{31}$$

and

$$\ddot{\varphi}_B = \frac{3}{\mu L_1\left(\frac{L_1}{2}+\frac{2L_2}{3}\right)}\left(\frac{M_0}{L_1\sqrt{1+(T_0\dot{\varphi}_B/M_0\dot{\vartheta}_B)^2}} - \frac{2T_0\left(L_1+\frac{1}{3}L_2\right)}{L_2^2\sqrt{1+(M_0\dot{\vartheta}_3/T_0\dot{\varphi}_B)^2}}\right) \tag{32}$$

Eqs. (31) and (32) can be solved by applying a fourth order Runge-Kutta method. Phase IV ends at τ_{IV} when $\dot{\vartheta}_B=\dot{\varphi}_B=0$ and the beam ceases to move.

3. Numerical results

Numerical calculations have been carried out for all four phases of the response for different combinations of load magnitude, F and pulse duration, τ_1. The energy balance has been examined at the end of each phase by checking that the total energy supplied to the cantilever is equal to the sum of the energy dissipated in the plastic hinges and the remaining kinetic energy of the beam. In calculations the structural parameters were set at M_0=316Nm, T_0/M_0=0.9, μ=2.662 kg/m, L_1=1m and L_2=2m based on a specimen of 2.45cm bore mild steel seamless tube. The rotation angle at H_1 due to bending at the end of Phase I was maintained at no more than 0.16rad, i.e., less than 10° in order not to invalidate the small deflection assumption under which the study was carried out.

Fig. 5 shows hinge positions at various times and the ratio T/M at each hinge plotted against hinge position for a typical case with F=2000N and τ=0.01sec. The ratio T/M increases when the hinge moves towards root B, indicating that torsion becomes more and more dominant in the response.

For the above case, the history of tip deflection to the final tip deflection and percentage of energy dissipated in each phase to the total input energy are shown in Fig. 6. More than half of the input energy is consumed during Phases I and II. It is noticed that the energy dissipated in Phase I, the stationary hinge phase, is quite close to one third of the total energy supplied to the structure, similar to solutions of a bent cantilever with its bend angle not equal $\pi/2$ (Reid, Wang and Hua 1995).

Table 1 reveals the influence of pulse characteristics on the overall response of a right-angled bent beam, the higher the load, the farther the hinges are from the bend, and the closer the energy

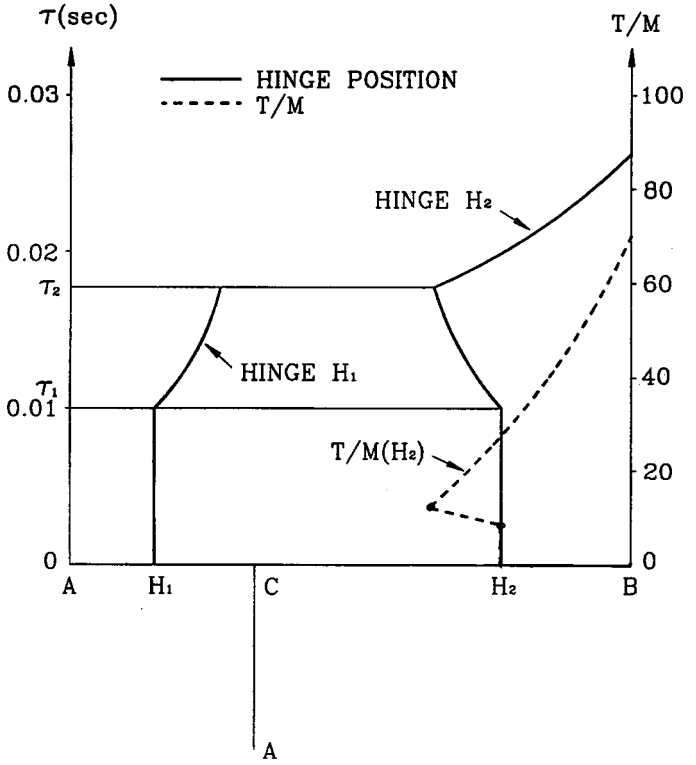

Fig. 5 Hinge positions at various time and the ratio T/M at each hinge against hinge position. F=2000 N and τ_1=0.001 sec, beam parameters are listed in Table 1

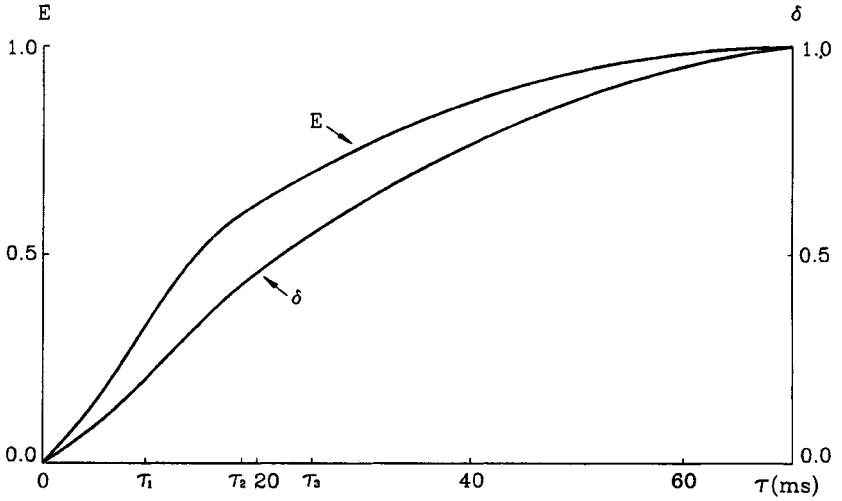

Fig. 6 Percentage of the tip deflection and input energy dissipated in each phase, beam parameters are listed in Table 1

dissipating ratio in Phase I to 1/3. Fig. 7 shows the final tip deflection δ_A and the total response time τ_f for various values of F while τ_1 is kept constant. The relationship between τ_f and F is

Table 1 Influence of load magnitude on structural response

F(N)	τ_1(sec)	x_1(m)	x_2(m)	E_I(%)	E_{II}(%)	E_{III}(%)	E_{IV}(%)	τ_f(sec)	δ_A(m)
1500	0.012	0.566	1.043	31.5	12.4	21.1	35.0	0.063	0.561
2000	0.007	0.454	1.313	33.0	26.2	14.1	26.1	0.049	0.384
3000	0.004	0.312	1.654	33.3	39.9	8.7	18.1	0.042	0.329

Note: structural parameters are M_0=316 Nm, T_0/M_0=0.9, $\beta=\pi/2$, μ=2.662 kg/m, L_1=1 m, L_2=2 m. x_1 and x_2 represent hinge position of H_1 and H_2 during Phase I, respectively. E_i, i=*I-IV*, are the percentages of energy dissipated in each phase to the total input energy. τ_f is the final response time. δ_A is the final deflection of beam tip.

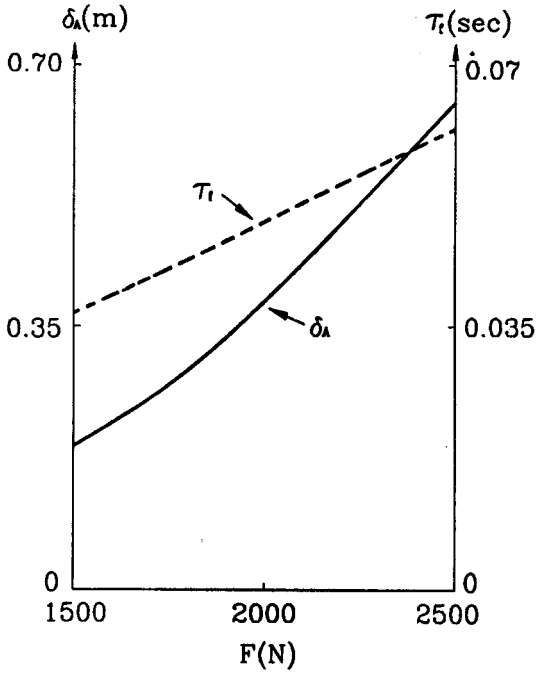

Fig. 7 The final tip deflection and the total response time against values of F with τ_1= 0.007 sec, beam parameters are listed in Table 1

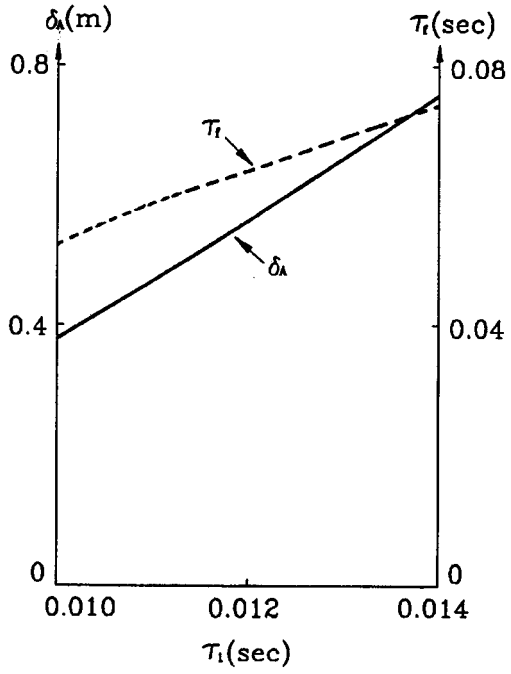

Fig. 8 The final tip deflection and the total response time against values of τ_1 with F= 1500 N, beam parameters are listed in Table 1

almost linear and δ_A increases rapidly with increasing magnitude of F. When load F is kept constant and changes are made to the pulse duration τ_1, similar results are obtained, as illustrated in Fig. 8.

4. Discussions

The transient response of a group of right angled bent cantilevers under an out-of-plane rectangular pulse has been analysed and it shows a four-phase response. Checks have been made to verify that the yield conditions are not violated in each segment of the beam and during each

phase of the response examined herein.

Numerical results show that the energy dissipated at the stationary hinges (Phase I) is close to one third of the total input energy and hinge velocities are not constant during the following traveling phases. Segment AC bears the most severe deformation due to bending. The deformation in CB is relatively small and when the load magnitude increases it reduces.

An important distinction between the cases of the bend angle $\beta=\pi/2$ and those with $\beta\neq\pi/2$ discussed by Reid, Wang and Hua (1995) is that whereas bending becomes dominant eventually in the latter case, torsion dominates phases III and IV for $\beta=\pi/2$. This is shown in Fig. 6. While hinge H_2 runs towards B, the ratio T/M at the hinge increases rapidly. Thus one would expect different failure mechanisms in these cases.

The work presented in this paper, based on a rigid-perfectly plastic material model, provides for a complete transient solution for bent cantilevers of right angle subjected to out-of-plane force pulses. The solution satisfies both static and kinematic conditions, i.e., the yield criterion and governing equations. But similar to many other works, the solution is restricted to small deflections. It would be a significant improvement to see an analysis which can not only provide complete solutions, but also be able to model the complexity of large deflections resulting from combined bending and torsional deformations.

References

Hua, Y. L., Yu, T. X. and Reid, S. R. (1988), "Double-hinge modes in the dynamic response of plastic cantilever beams subjected to step loading", *Int. J. Impact Engng.*, **7**, 401-413.

Martin, J. B. (1964), *The Permanent Deformation of a Bent Cantilever*, Division of Engineering, Brown University Report N87 GP 1115/15.

Parkes, E. W. (1955), "The permanent deformation of a cantilever struck transversely at its tip", *Pro. of Royal Society, Series A*, **228**, 462-476.

Reid, S. R., Wang, B. and Yu, T. X. (1995), "Yield mechanisms of a bent cantilever beam subjected to a suddenly applied constant out-of-plane force", *Int. J. Impact Engng.*, **16**, 49-73.

Reid, S. R., Wang, B. and Hua, Y. L. (1995), "Triple plastic hinge mechanisms for a bent cantilever beam subjected to an out-of-plane tip force pulse of finite duration", *Int. J. Impact Engng.*, **16**, 75-93.

Wang, B. (1994), "Response of a bent cantilever to an impulsive load applied at its tip normal to its plane", *Int. J. Solids Structures*, **31**, 1377-1392.

Appendix

Derivation of governing equations of Phase II

(1) Segment H_1CH_2

Supposing that P_1 and P_2 are arbitrary points in H_1C and CH_2, respectively, as shown in Fig. A1. Their velocities may be expressed as

$$V_{P_2}=-(x_2-\lambda_2)\dot{\vartheta}_2$$

and

$$V_{P_1}=\lambda_1\dot{\varphi}_2-x_2\,\dot{\vartheta}_2$$

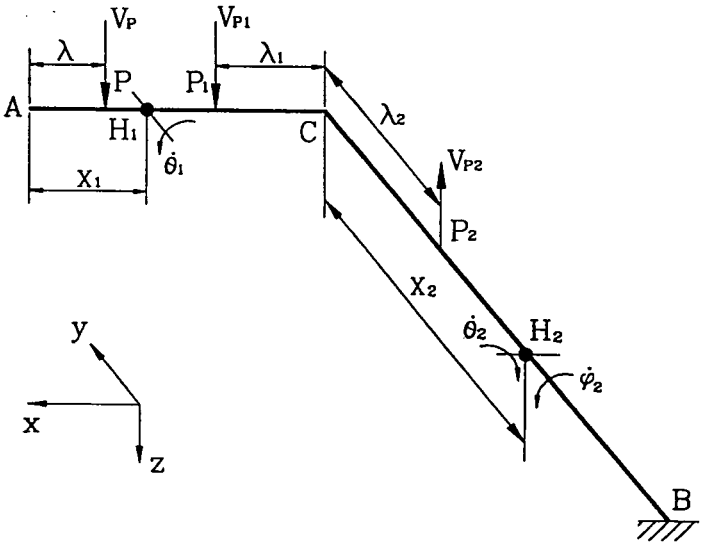

Fig. A1 The variables in phase II

The corresponding accelerations are

$$a_{P_2}=-(x_2-\lambda_2)\,\ddot{\vartheta}_2-\dot{x}_2\,\dot{\vartheta}_2$$

and

$$a_{P_1}=\lambda_1\ddot{\varphi}_2-\dot{x}_2\dot{\vartheta}_2-x_2\ddot{\vartheta}_2.$$

The equation of translational motion for segment H_1CH_2 is

$$0=\int_0^{L_1-x_1}\mu a_{P_1}d\lambda_1+\int_0^{x_2}\mu a_{P_2}d\lambda_2$$

$$=\frac{\mu}{2}(L_1-x_1)^2\,\ddot{\varphi}_2-\mu(L_1-x_1)x_2\ddot{\vartheta}_2-\mu(L_1-x_1)\dot{x}_2\dot{\vartheta}_2-\frac{\mu}{2}x_2^2\,\ddot{\vartheta}_2-\mu x_2\dot{x}_2\,\dot{\vartheta}_2 \tag{A1}$$

The rotational equation of motion about axis CB is

$$M_0-T_2=\int_0^{L_1-x_1}\mu\lambda_1 a_{P_1}d\lambda_1$$

$$=\frac{\mu}{3}(L_1-x_1)^3\ddot{\varphi}_2-\frac{\mu}{2}(L_1-x_1)^2x_2\ddot{\vartheta}_2-\frac{\mu}{2}(L_1-x_1)^2\dot{x}_2\dot{\vartheta}_2 \tag{A2}$$

where the rotational inertia of segment OH_2 is neglected.

The rotational motion about axis AC is governed by

$$-M_2=\int_0^{x_2}\mu\lambda_2 a_{P_2}d\lambda_2$$

or

$$M_2=\frac{\mu}{6}x_2^3\,\ddot{\vartheta}_2+\frac{\mu}{2}x_2^2\dot{x}_2\dot{\vartheta}_2 \tag{A3}$$

(2) Segment AH_1

Let P be an arbitrary point in AH_1. The velocity of point P is

$$V_P = (x_1 - \lambda)\ \dot{\vartheta}_1 + (L_1 - \lambda)\ \dot{\varphi}_2 - x_2 \dot{\vartheta}_2$$

and the acceleration is

$$a_P = (x_1 - \lambda)\ \ddot{\vartheta}_1 + (L_1 - \lambda_1)\ \ddot{\varphi} - x_2\ \ddot{\vartheta}_2 + \dot{x}_1\ \dot{\vartheta}_1 - \dot{x}_2\ \dot{\vartheta}_2.$$

The translational equation of motion for segment AH_1 is

$$0 = \int_0^{x_1} \mu a_P\, d\lambda$$

$$= \frac{\mu}{2} x_1^2\ \ddot{\vartheta}_1 + \mu \left(L_1 - \frac{x_1}{2} \right) x_1\ \ddot{\varphi}_2 - \mu x_1 x_2\ \ddot{\vartheta}_2 + \mu x_1 \dot{x}_1 \dot{\vartheta}_1 - \mu x_1 \dot{x}_2\ \dot{\vartheta}_2 \tag{A4}$$

The rotational motion of AH_1 about point A is described by

$$M_0 = \int_0^{x_1} \mu \lambda a_P\, d\lambda$$

$$= \frac{\mu}{6} x_1^3\ \ddot{\vartheta}_1 + \mu \left(\frac{L_1}{2} - \frac{x_1}{3} \right) x_1^2\ \ddot{\varphi}_2 - \frac{\mu}{2} x_1^2 x_2\ \ddot{\vartheta}_2 + \frac{\mu}{2} x_1^2 \dot{x}_1\ \dot{\vartheta}_1 + \frac{\mu}{2} x_1^2 \dot{x}_2\ \dot{\vartheta}_2 \tag{A5}$$

At hinge H_2, the yielding condition and flow rule are

$$\left(\frac{M_2}{M_0} \right)^2 + \left(\frac{T_2}{T_0} \right)^2 = 1 \quad \text{and} \quad \dot{\varphi}_2 = \left(\frac{M_0}{T_0} \right)^2 \frac{T_2}{M_2}\ \dot{\vartheta}_2.$$

The above equations can then be re-organized into a form suitable for numerical solution as listed in Eqs. (16) to (20).